Journal of Sound and Vibration (1998) **209**(3), 419–442

ON THE FLEXURAL VIBRATION OF TIMOSHENKO BEAMS, AND THE APPLICABILITY OF THE ANALYSIS TO A SANDWICH CONFIGURATION

M. R. Maheri and R. D. Adams

Department of Mechanical Engineering, University of Bristol, Queen's Building, University Walk, Bristol, BS8 1TR, England

(*Received* 24 *September* 1993, *and in final form* 21 *July* 1997)

The viability of adapting the Timoshenko beam equations to a sandwich configuration is considered. These equations are utilised for modal analysis of solid as well as sandwich beams, including beams with a mass attached at the mid-span. Theoretical and experimental results regarding beam frequencies and mode shapes are presented.

1. INTRODUCTION

The flexural vibration of centrally loaded† beams is of particular interest in the steady state measurement of damping since, in the forced vibration of beams, it may be required that the latter is loaded at its mid-point by the drive and/or pick-up mechanisms [1]. Of particular relevance in this respect are beams with sandwich configuration [2]. Since these are light but very stiff in flexure, the drive mechanism could be relatively heavy and this could considerably change the frequency and mode shape of the beam.

A simple adaptation of the Timoshenko beam equations to a damped sandwich configuration has been reported previously [3]. Whereas a considerable amount of literature exists on Timoshenko beam theory, perhaps surprisingly, very few experimental investigations of the analysis have been undertaken [4]. The aim of the work reported here was to examine the viability of adapting the Timoshenko beam equations to flexural vibration of sandwich beams, including beams with an attached mass. To that end, a series of modal tests was conducted on both solid and sandwich beams. The results were compared with those predicted by the Timoshenko equations and the proposed adaptation of these equations for a sandwich configuration. As is normally the practice in the measurement of material damping, only free-free beams were considered.

2. GOVERNING EQUATIONS

The coupled equations with respect to the total lateral deflection, w, and the bending slope, ϕ, of a Timoshenko beam are given as [5]

$$EI\frac{\partial^2\phi}{\partial x^2}+k\left(\frac{\partial w}{\partial x}-\phi\right)AG-\rho I\frac{\partial^2\phi}{\partial t^2}=0, \qquad \rho A\frac{\partial^2 w}{\partial t^2}-k\left(\frac{\partial^2 w}{\partial x^2}-\frac{\partial\phi}{\partial x}\right)AG=0, \quad \text{(1a, b)}$$

†The terms "load" and "loaded" are somewhat loosely used here; but they are used for conciseness and refer to a mass attached to the beam.

0022–460X/98/030419 + 24 $25.00/0/sv971278

where

$$w = W\,e^{i\omega t}, \qquad \phi = \Phi\,e^{i\omega t}, \tag{2, 3}$$

and W and Φ are normal functions of x. (A list of nomenclature is given in the Appendix.)

Eliminating, in turn, ϕ and w from equations (1) yields the two uncoupled differential equations of flexure [6]:

$$EI\frac{\partial^4 w}{\partial x^4} + \rho A\frac{\partial^2 w}{\partial t^2} - \left(\rho I + \frac{E\rho I}{kG}\right)\frac{\partial^4 w}{\partial x^2\,\partial t^2} + \frac{\rho^2 I}{kG}\frac{\partial^4 w}{\partial t^4} = 0, \tag{4a}$$

$$EI\frac{\partial^4 \phi}{\partial x^4} + \rho A\frac{\partial^2 \phi}{\partial t^2} - \left(\rho I + \frac{E\rho I}{kG}\right)\frac{\partial^4 \phi}{\partial x^2\,\partial t^2} + \frac{\rho^2 I}{kG}\frac{\partial^4 \phi}{\partial t^4} = 0. \tag{4b}$$

By substituting for ϕ and w from equations (2) and (3) in equations (1) and (4), the latter are respectively reduced to

$$s^2\frac{\partial^2 \Phi}{\partial \zeta^2} - (1 - b^2r^2s^2)\Phi + \frac{1}{L}\frac{\partial W}{\partial \zeta} = 0, \qquad \frac{\partial^2 W}{\partial \zeta^2} + b^2s^2W - L\frac{\partial \Phi}{\partial \zeta} = 0, \tag{5a, b}$$

$$\frac{\partial^4 W}{\partial \zeta^4} + b^2(r^2 + s^2)\frac{\partial^2 W}{\partial \zeta^2} - b^2(1 - b^2r^2s^2)W = 0 \tag{6a},$$

$$\frac{\partial^4 \Phi}{\partial \zeta^4} + b^2(r^2 + s^2)\frac{\partial^2 \Phi}{\partial \zeta^2} - b^2(1 - b^2r^2s^2)\Phi = 0, \tag{6b}$$

where

$$\zeta = x/L, \qquad b^2 = \rho AL^4\omega^2/EI, \qquad r^2 = I/AL^2, \qquad s^2 = EI/kAGL^2 \tag{7–10}$$

The solutions of equations (6) are

$$W = C_1\cosh(b\alpha\zeta) + C_2\sinh(b\alpha\zeta) + C_3\cos(b\beta\zeta) + C_4\sin(b\beta\zeta), \tag{11a}$$

$$\Phi = C_1'\sinh(b\alpha\zeta) + C_2'\cosh(b\alpha\zeta) + (C_3'\sin(b\beta\zeta) + C_4'\cos(b\beta\zeta), \tag{11b}$$

where

$$\alpha, \beta = (1/\sqrt{2})\{-, +(r^2 + s^2) + [(r^2 - s^2)^2 + 4/b^2]^{1/2}\}^{1/2} \tag{12}$$

are roots of the biquadratic characteristic equation.

Only half of the coefficients C_i, C_i', $(i = 1, 2, 3, 4)$ are independent, since W and Φ are coupled by equations (1). The dependent coefficients are found by substituting equations (11) in either one of the coupled equations (5) and equating the coefficients of individual hyperbolic and trigonometric terms. The following are found from equation (5b):

$$C_1' = \frac{b}{L}\left(\frac{\alpha^2 + s^2}{\alpha}\right)C_1, \qquad C_2' = \frac{b}{L}\left(\frac{\alpha^2 + s^2}{\alpha}\right)C_2, \qquad C_3' = -\frac{b}{L}\left(\frac{\beta^2 - s^2}{\beta}\right)C_3,$$

$$C_4' = \frac{b}{L}\left(\frac{\beta^2 - s^2}{\beta}\right)C_4. \tag{13}$$

Equations (11) and their first derivatives may now be written as

$$W = C_1 \cosh(b\alpha\zeta) + C_2 \sinh(b\alpha\zeta) + C_3 \cos(b\beta\zeta) + C_4 \sin(b\beta\zeta), \tag{14a}$$

$$\partial W/\partial x = (b/L)\,[C_1\,\alpha \sinh(b\alpha\zeta) + C_2\,\alpha \cosh(b\alpha\zeta) - C_3\,\beta \sin(b\beta\zeta) + C_4\,\beta \cos(b\beta\zeta), \tag{14b}$$

$$\Phi = \frac{b}{L}\left[\frac{\alpha^2 + s^2}{\alpha}(C_1 \sinh(b\alpha\zeta) + C_2 \cosh(b\alpha\zeta)) - \frac{\beta^2 - s^2}{\beta}(C_3 \sin(b\beta\zeta) - C_4 \cos(b\beta\zeta))\right], \tag{14c}$$

$$\partial\Phi/\partial x = (b/L)^2[(\alpha^2 + s^2)(C_1 \cosh(b\alpha\zeta) + C_2 \sinh(b\alpha\zeta)) - (\beta^2 - s^2)(C_3 \cos(b\beta\zeta) + C_4 \sin(b\beta\zeta))]. \tag{14d}$$

3. CENTRALLY LOADED BEAM

A free–free Timoshenko beam carrying a point mass M_c at the mid-span (see Figure 1) and vibrating in a symmetric normal mode is subjected to the following conditions:

$$\text{(i) at } x = 0, \qquad EI\frac{\partial\Phi}{\partial x} = 0 \quad \text{(zero bending moment), so } \frac{\partial\Phi}{\partial x} = 0, \tag{15a}$$

$$\text{(ii) at } x = 0, \qquad kAG\gamma = 0 \quad \text{(zero shearing force), so } \left(\frac{\partial W}{\partial x} - \Phi\right) = 0, \tag{15b}$$

$$\text{(iii) at } x = L/2, \qquad \Phi = 0 \quad \text{(zero bending slope);} \tag{15c}$$

$$\text{(iv) at } x = L/2, \qquad kAG\gamma - (M_c/2)\omega^2 W = 0 \quad \text{(shear force induced due to } M_c\text{)},$$
$$\text{so } kAG(\partial W/\partial x - \Phi) - (M_c/2)\omega^2 W = 0, \qquad \text{or} \qquad kAG(\partial W/\partial x) - (M_c/2)\omega^2 W = 0. \tag{15d}$$

Equations (15) respectively give the four equations

$$C_1(\alpha^2 + s^2) - C_3(\beta^2 - s^2) = 0, \qquad -C_2\,\beta + C_4\,\alpha = 0, \tag{16a, b}$$

$$\beta(\alpha^2 + s^2)(C_1 \sinh(H) + C_2 \cosh(H)) - \alpha(\beta^2 - s^2)(C_3 \sin(T) + C_4 \cos(T)) = 0, \tag{16c}$$

$$(mL/b^2 s^2)(b/L)\,[C_1\,\alpha \sinh(H) + C_2\,\alpha \cosh(H) - C_3\,\beta \sin(T) + C_4\,\beta \cos(T)] - (M_c/2)\,[C_1 \cosh(H) + C_2 \sinh(H) + C_3 \cos(T) + C_4 \sin(T)] = 0, \tag{16d}$$

where $H = b\alpha/2$ and $T = b\beta/2$.

Equations (16) may be written in the form $[A]\{C_i\} = 0$, $i = 1, 2, 3, 4$. For a non-trivial solution, the determinant of the matrix of coefficients $[A]$ is set to zero. This will give the

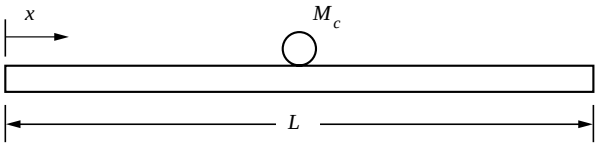

Figure 1. Centrally loaded beam.

following frequency equation for the symmetric modes of the centrally loaded free–free Timoshenko beam:

$$\frac{(\alpha^2+s^2)^2+(\beta^2-s^2)^2}{\beta(\alpha^2+s^2)(\beta^2-s^2)}\cot(T)\frac{M_c}{2}-\frac{(\beta^2-\alpha^2)}{\alpha\beta^2}\tanh(H)\frac{M_c}{2}$$
$$+\frac{(\alpha^2+\beta^2)}{\alpha\beta(\alpha^2+s^2)}\frac{m}{b}\cot(T)\tanh(H)+\frac{M_c}{\beta\sin(T)\cosh(H)}+\frac{(\alpha^2+\beta^2)}{\beta^2(\beta^2-s^2)}\frac{m}{b}=0. \quad (17a)$$

For the anti-symmetric modes, the boundary conditions (i) and (ii) in equations (15) still apply; but the boundary conditions (iii) and (iv) in those equations should be replaced by their following counterparts:

$$\text{(iii) at } x=L/2, \qquad W=0 \text{ (zero lateral deflection);}$$

$$\text{(iv) at } x=L/2,$$

$$EI(\partial\Phi/\partial x)+(J/2)\omega^2(\partial W/\partial x)=0 \text{ (bending moment due to rotary inertia of mass).}$$

By a procedure similar to that for the symmetric modes above, it can be shown that these four boundary conditions will give the following frequency equation for the anti-symmetric modes of the centrally loaded free-free Timoshenko beam:

$$(\alpha/\beta)(\alpha^2+\beta^2)(\alpha^2+s^2)\cot(T)-(\beta^2-s^2)(\alpha^2+\beta^2)\coth(H),$$
$$+\left(\frac{1}{\beta}\right)((\alpha^2+s^2)\alpha^2+(\beta^2-s^2)\beta^2)\frac{Jb}{2mL^2}\cot(T)\coth(H)$$
$$+\left(\frac{1}{\beta}\right)((\alpha^2+s^2)\beta^2+(\beta^2-s^2)\alpha^2)\frac{Jb}{2mL^2}\frac{1}{\sin(T)\sinh(H)}$$
$$+\alpha(\alpha^2-\beta^2+2s^2)\frac{Jb}{2mL^2}=0. \quad (17b)$$

From equations (16), three of the constants C_i may be found in terms of the fourth one, for example C_3, giving, from equation (14a), the total lateral deflection, W, as

$$W=\frac{\beta^2-s^2}{\alpha^2+s^2}C_3\cosh(b\alpha\zeta)+\frac{P}{\beta}C_3\sinh(b\alpha\zeta)+C_3\cos(b\beta\zeta)+\frac{P}{\alpha}C_3\sin(b\beta\zeta), \quad (18)$$

where

$$P=\frac{(\beta^2-s^2)(\alpha\sin(T)-\beta\sinh(H))}{(\beta^2-s^2)\cos(T)+(\alpha^2+s^2)\cosh(H)}. \quad (19)$$

Now, if W is known at some positive value of x, then C_3 can be found from equation (18). Consequently, the constants C_1, C_2 and C_4 will be known, and the quantities W, $\partial W/\partial x$, Φ and $\partial\Phi/\partial x$ can be found explicitly for any x.

The Timoshenko beam equations are readily simplified to the elementary Bernoulli–Euler beam equations by setting to zero r and s, the rotary inertia and the shear parameters.

4. SANDWICH BEAMS

It has been suggested that by following a simple procedure, it should be possible to adapt the Timoshenko beam equations for a symmetric skin-core-skin sandwich beam [3]. To that end, the following usual assumptions are made [7–10]: (1) the in-plane modulus of the core is negligible compared to that of the skin; (2) the transverse shear deflection of the skin is negligible compared to that of the core. By virtue of the first assumption, the bending stiffness EI in equations (8) and (10) will be that of the skins about the sandwich mid-plane. In accordance with the Timoshenko beam equations, this implies that the skins bend about the sandwich neutral axis and, therefore, undergo uniaxial tension or compression. From assumption (2), the area A will be the cross-sectional area of the core only. The rotary inertia parameter r, is now expressed in terms of I_s, the effective moment of inertia of the whole beam cross-section. Based on these assumptions, equations (8)–(10) can be written as

$$b^2 = mL^3\omega^2/(EI)_s, \qquad r^2 = I_{sc}/A_c L^2, \qquad s^2 = (EI)_s/(kAG)_c L^2, \tag{20–22}$$

where suffixes s and c indicate skin and core respectively, and I_{sc} is given by

$$I_{sc} = I_s + (\rho_c/\rho_s)I_c. \tag{23}$$

4.1. THE SHEAR CORRECTION FACTOR, k

The question arises as to the value of the factor k (equation (22)), following the above procedure. The first of the above assumptions implies that the shear distribution over the core cross-section is uniform [9], which in turns leads to a shear correction factor of unity. However, the notion of unity of the factor k which follows the assumed uniformity of shear distribution over the core cross-section would be somewhat misleading, since it ignores the shearing stresses which must exist in the skins if the implication of shear discontinuity at the interface is to be avoided [11]. On the other hand, if it is assumed that the shear stress over the whole sandwich cross-section is uniform, then this implies that the shear stress in the skin is of the same order as that in the core, regardless of the core shear rigidity. As pointed out by Mead [12], this cannot be the case when the core is soft, in which case the skins tend to bend independently of the core and about their own neutral axis.

An assumption which is implicit within the Timoshenko beam equations is that no through-thickness normal strain in the beam occurs, such that the outmost planes, for example, remain at the same fixed distance apart, regardless of the state of the stress. This assumption is not exclusive to the Timoshenko equations as it also underlies the classical theory of bending. Since, in a sandwich configuration, the core normally has a relatively small elastic modulus, the assumption imposes a constraint on the deformation in that it allows no localized bending of the skins which can be caused by a point load. It has been shown, in the case of solid beams, that for a length along the beam approximately equal to half of the depth of the beam, there exists an additional curvature due to a point load [13]. Similarly, the state of stress within the skins is also assumed to be unaffected by any transverse compressive stresses which may develop in the core.

Moreover, when the beam is subjected to dynamic loading, the rotary inertia effects could become the determining factors in the shear distribution [14, 15], although this is expected to occur only at high frequencies.

From the foregoing, it becomes apparent that an analytical determination of the shear correction factor for a sandwich configuration, and in particular for point loaded beams, not only is difficult but, strictly speaking, for any given beam and boundary conditions, there exists a unique correction factor attributable to each frequency of the beam. This

TABLE 1

Specifications of solid beams

Designation	Material	m (g)	L (mm)	w (mm)	h (mm)	E (GPa)	v
AL1	Duralumin	257·2	600·0	12·65	12·65	67·34	0·35
AL2	Duralumin	292·1	600·5	19·00	9·50	69·88	0·35

could, at least in part, explain the fact that a wide range of values has been quoted in the literature [3, 16].

In the present work, the authors propose to follow the practical approach suggested by Mindlin and Goodman [14, 15], and use a correction factor which best fits the experimental results at the high end of the frequency spectrum. The reason for using the high frequency end is based on the argument that the shear distribution at higher frequencies is more representative of the dynamic shear distribution in the beam. Clearly, a factor so found would no longer be limited to representing the form of the shear distribution as underlies the original Timoshenko theory, but rather would simply become an empirically obtained correction factor.

At this point, the authors wish to acknowledge the worthy contribution to this work made by Professor D. J. Mead. In a series of personal communications, he in particular made some interesting points regarding the nature of a Timoshenko type correction factor in a sandwich configuration. He suggests that the usual sandwich assumptions will, in fact, result in a relationship for the factor k of the form $k = 1 + t/c$. Furthermore, he finds that with this value of k, the Timoshenko predictions for the low and high mode frequencies of a simply supported sandwich beam will agree with the predictions by the "exact" Ross–Kerwin–Ungar equations. The suggested relationship for the factor k is in agreement with the empirical results of the present work only in the limiting case when $t/c \to 0$ (section 5.1, Figure 11), a fact that, he contends, can be attributed to the different nature of the deformation of cross-section between the solid Timoshenko beams and the sandwich beams and, therefore, the different nature of the rotary inertia parameter in each case. He, therefore, suggests that within the context of the present theoretical basis, a *rotary inertia* correction factor would also be in order for a sandwich beam, and that an empirically obtained correction factor would, in effect, embody both the shear as well as the rotary inertia correction factors.

5. EXPERIMENTAL PROCEDURE AND RESULTS

Solid beams of two different cross-sections were investigated. The specifications of was these solid beams, including elastic properties, are given in Table 1. The Young's modulus was found from the resonance flexural frequency of slender beam samples, and the Poisson's ratio for aluminium was assumed to be 0·35.

The sandwich beams were prefabricated, symmetric, all-aluminium beams using identical skin, core and adhesive. The specifications of the sandwich beams are given in Table 2. The manufacturer's quoted figure for the Young's modulus of the skin was used. The shear modulus of the honeycomb core was found by using the method described in reference [17]. The shear modulus was measured along the ribbon direction since this was the orientation of the core in all the sandwich beams tested.

TABLE 2

Specifications of the sandwich beams

Designation	m (g)	L (mm)	w (mm)	t (mm)	c (mm)	Cell size* (mm)	E_s (GPa)	G_c (GPa)
SB1	72·2	400·0	40·0	0·57	12·5	6·25	69	0·285
SB2	87·2	400·0	40·0	0·57	25·0	6·25	69	0·285
SB3	67·4	270·0	39·5	0·57	33·5	6·25	69	0·285
SB4	120·9	400·0	40·0	0·57	50·0	6·25	69	0·285

†The cell size refers to the diameter of the inscribed circle of the hexagonal honeycomb cell.

5.1. NATURAL FREQUENCIES

The frequency tests were carried out to the limits of the sensitivity of the equipment available. For greater accuracy, as far as it was possible the steady state technique was used, with an electrodynamic shaker for excitation. Beyond the frequency limit of the shaker (about 5 kHz), the transient technique was used, with particular care taken to tap the sample on the centre so as not to excite any torsional frequencies. The test set-up for the latter method is shown in Figure 2.

The frequency results are presented in Figures 3–11. For the solid beams, the predicted frequencies were obtained for a shear correction factor of 0·82, a figure which results from equating the first pure thickness-shear frequency of a Timoshenko beam with the first pure shear mode according to the exact three-dimensional theory of elasticity, as proposed by Mindlin [18]. For the sandwich beams, a value was selected for the correction factor which would closely predict (within $\pm 0.5\%$) the highest test frequency for each beam, as previously discussed. In both cases, the measured results are also compared with values calculated on the basis of zero shear deformation (here, simply referred to as "Bernoulli–Euler" results). For both the solid as well as the sandwich beams, the frequency results with unit correction factor are also included. These results, $F_{(k=1)}$, have also been used to normalize the difference between the measured frequency and the frequency predicted on the basis of a unit correction factor, namely

$$(F - F_{(k=1)})/F_{(k=1)}. \tag{24}$$

Furthermore, the frequencies are presented as functions of the mode number, this being the only common factor as far as the elementary Bernoulli–Euler and the Timoshenko theories are concerned.

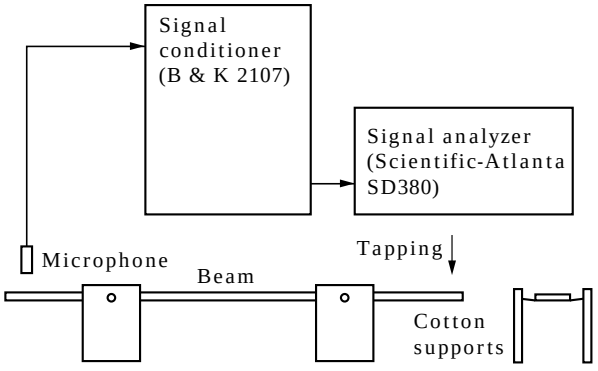

Figure 2. Transient measurement of natural frequencies.

For the solid beam results, generally good correlation exists between the frequencies predicted by the Timoshenko theory and the test results. Moreover, it can be seen that the accuracy of the prediction is maintained over the whole frequency range.

As can be seen (Figures 3 and 4), in the case of the solid unloaded beams, the difference between the predicted frequencies and the test results for either value of k is of any significance only at the highest frequencies. However, there does not seem to be any particular trend in the predictions regarding the two values of the shear factor. The observed deviations, in fact, are believed to be within the experimental limitations. Also, certain assumptions have been made regarding the elastic properties. A value for the Poisson's ratio, for example, has been assumed, and the shear modulus has been found by using this value. Furthermore, it is also likely that the anti-clastic curvature in the beam will influence the frequency as the half-wavelength approaches the beam width.

As expected, comapred to the results for the unloaded beams, there are some discrepancies in the frequency results of the centrally loaded solid beam (Figures 5(a) and (b)). The discrepancies are believed to have been caused by eccentricity of the point mass (the mass on the Duralumin beam was in the shape of a cylinder with a mass ratio to that of the beam of 0·38, and this was bonded along its length across the width of the beam so that a point-loading condition could be achieved). It is also noted that, with the in-plane rotary inertia effects of the centre mass neglected, the anti-symmetric frequencies of the centrally loaded and those of the unloaded beam will be the same since, in each case, the mid-span is laterally stationary. This can be verified by comparing the anti-symmetric frequency results in Figures 4 and 5(b). Up to the onset of the discrepancies (modes 2–12 (inclusive), Figure 5(b)), the two frequencies are found to be almost identical.

As is evident from Figure 5, with the loaded beams the fundamental frequency is generally underestimated by both values of $k = 1$ and 0·82, a possible indication of a difference in shear distribution, at least in the fundamental mode, between the loaded and unloaded beams.

The shear effect in shear-soft sandwich beams is much more profound, as can be seen by comparing the frequencies obtained by the elementary and the Timoshenko theories in Figures 6–10. The shear modulus of the solid beam AL1 is about 93 times greater than that of the aluminium honeycomb sandwich beam SB1, so the predicted frequencies of the latter are much more sensitive to the value of k which is used. For example, at the highest frequency which could be measured for the unloaded SB1 beam (mode 9, Figure 6), a change of k from 1·77 to 1·0 decreases the predicted frequency by some 25% while, in a solid beam and at a comparable mode number, a change of the same order in the value of k has almost no effect on the frequency.

In the case of the sandwich beams, although a value for k was selected so as to yield the highest test frequency the results, nevertheless, indicate a remarkable accuracy of the predictions over the entire frequency range attainable, especially for thicker beams (Figures 8–10). The frequencies of the centrally loaded beam (Figure 7) are also accurately predicted, although slightly more scatter of results is observed here (compare Figures 6 and 7).

The test results for the four unloaded beams varying only in the thickness of the core (Figures 6, 8–10) suggest that k is sensitive to the core thickness. Using these results, the optimun value of k has been considered as a function of the skin/core thickness ratio in Figure 11. The results in this figure suggest that k varies linearly

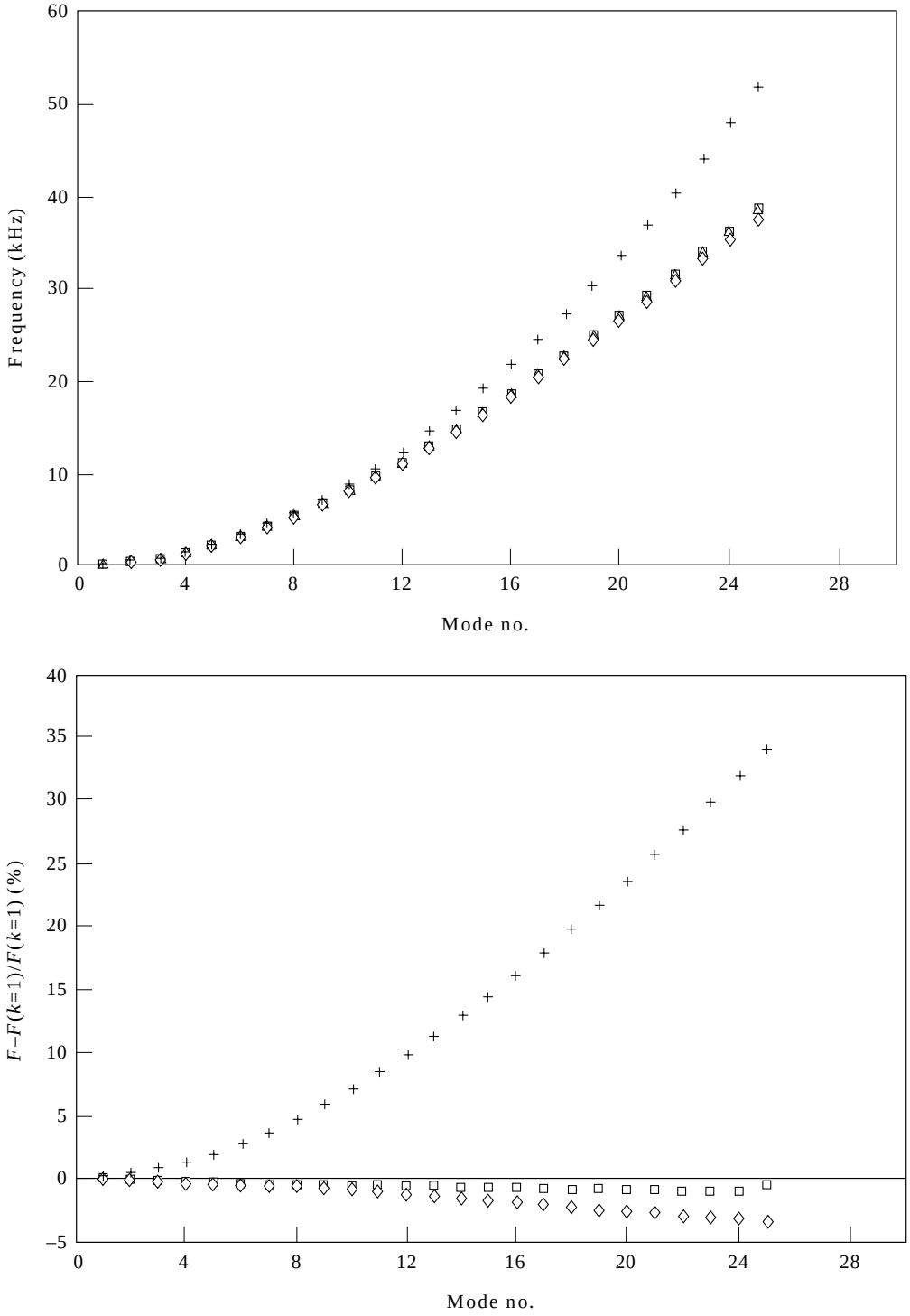

Figure 3. Frequency versus mode no. (test piece: AL1, square section Duralumin beam.) △, Timoshenko ($k = 1{\cdot}0$); ◇, Timoshenko ($k = 0{\cdot}82$), +, Bernouilli–Euler; □, test; ——, Timoshenko ($k = 1{\cdot}0$).

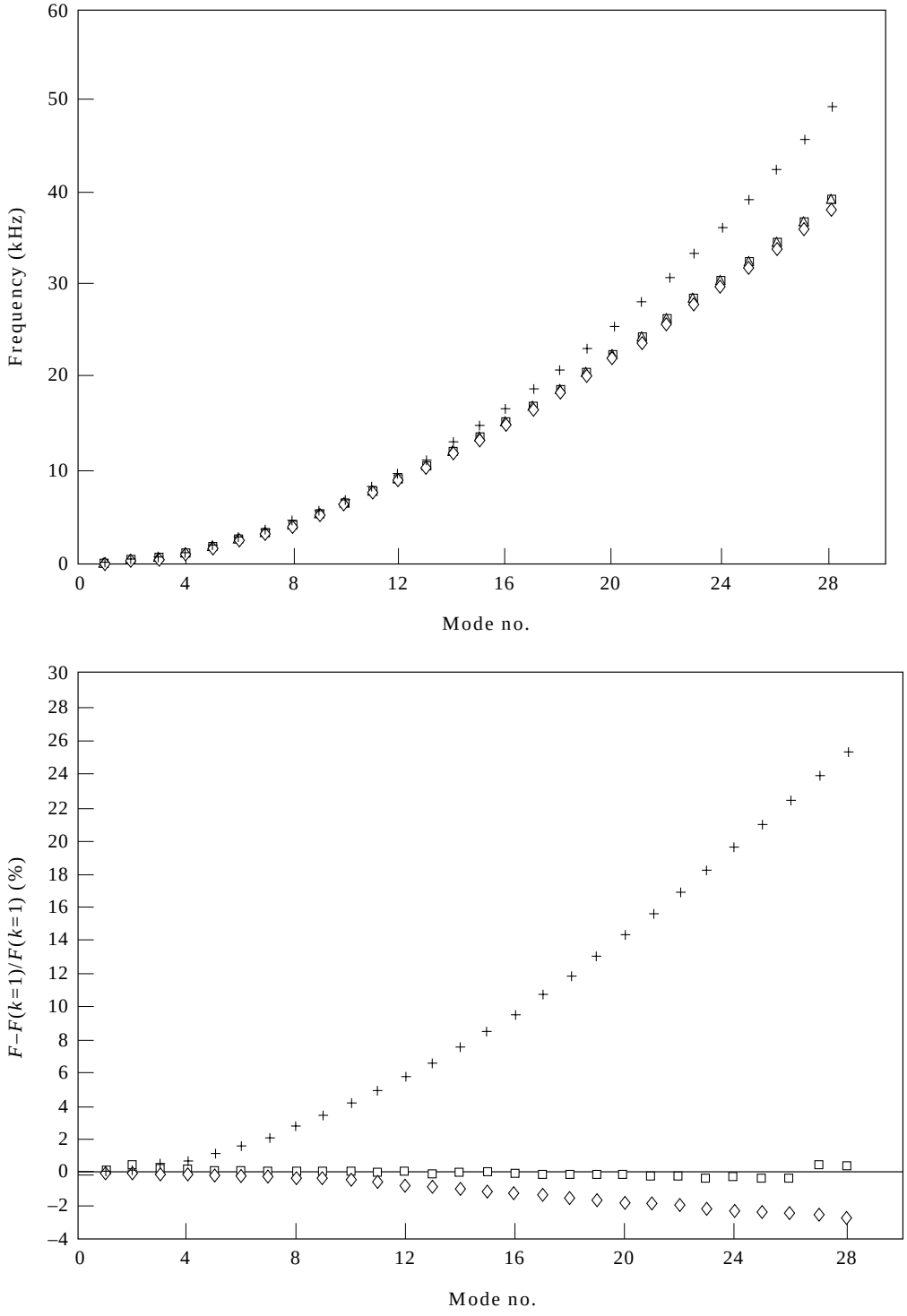

Figure 4. Frequency versus mode no. (test piece: AL2, rectangular section Duralumin beam.) △, Timoshenko ($k = 1{\cdot}0$); ◇, Timoshenko ($k = 0{\cdot}82$), +, Bernouilli–Euler; □, test; ——, Timoshenko ($k = 1{\cdot}0$).

(a)

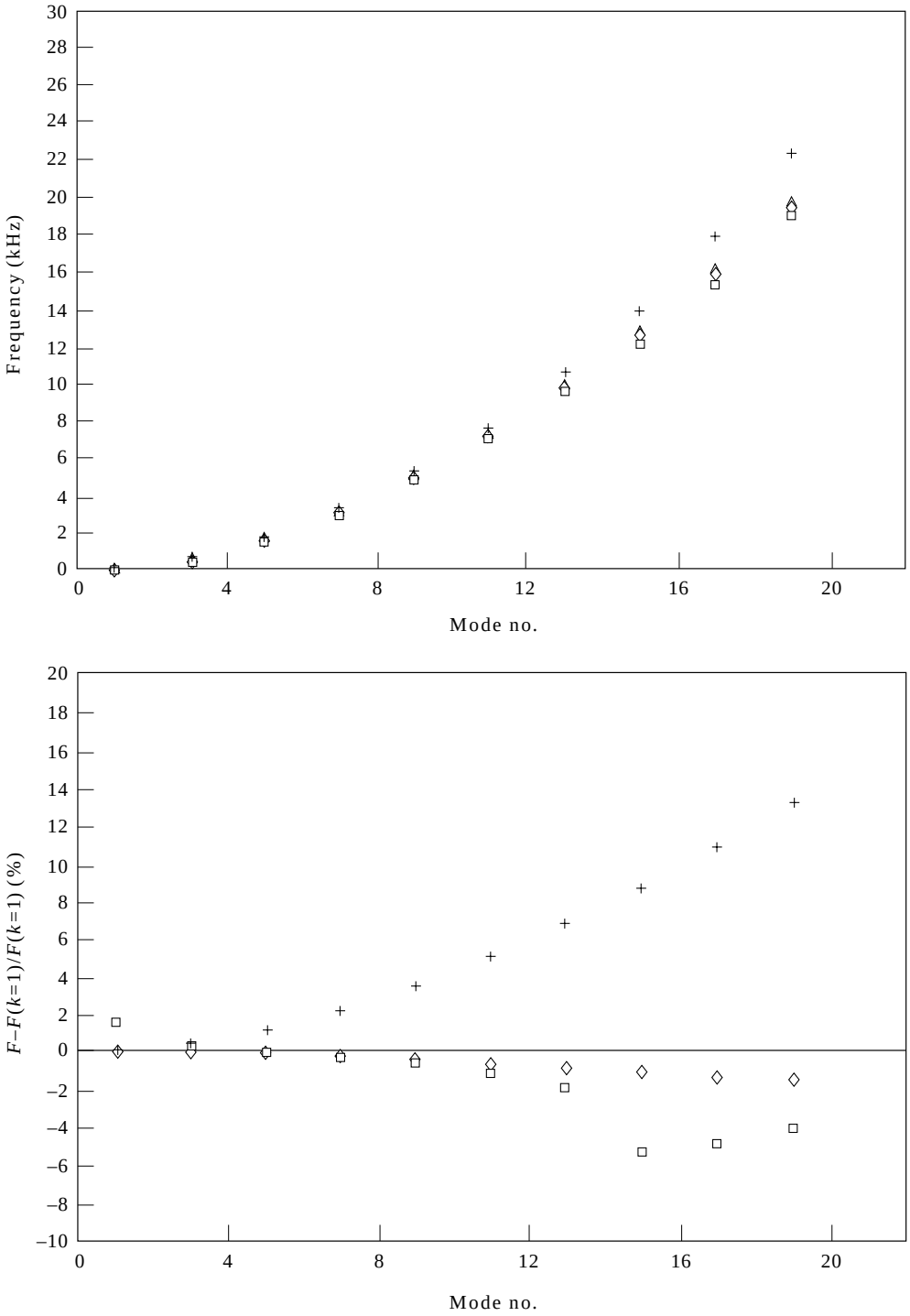

Figure 5(a)—(*caption overleaf*)

(b)

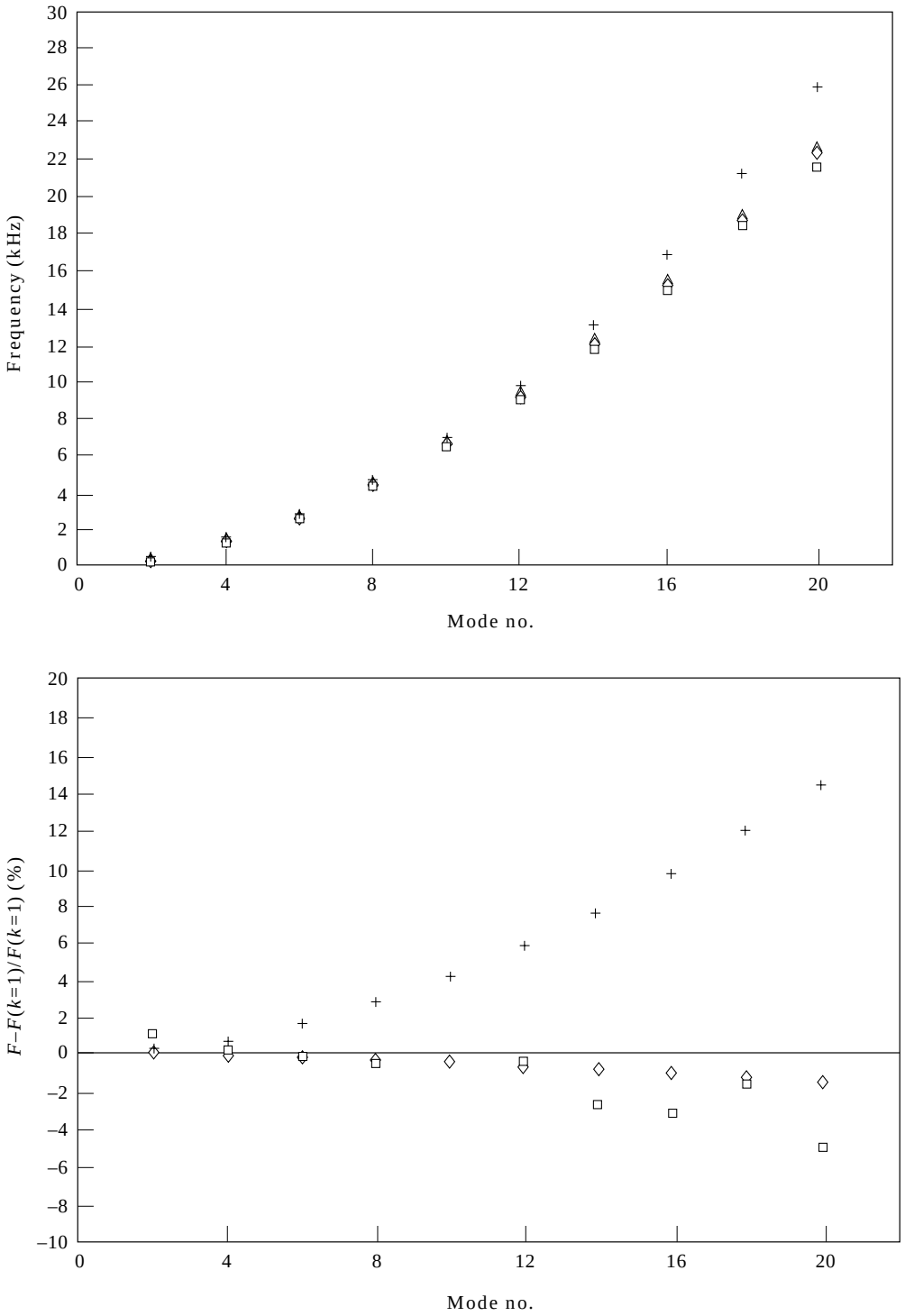

Figure 5. Frequency versus (a) symmetric modes and (b) antisymmetric modes. (test piece: centrally-loaded, AL2, rectangular section Duralumin beam.) Key as Figure 3.

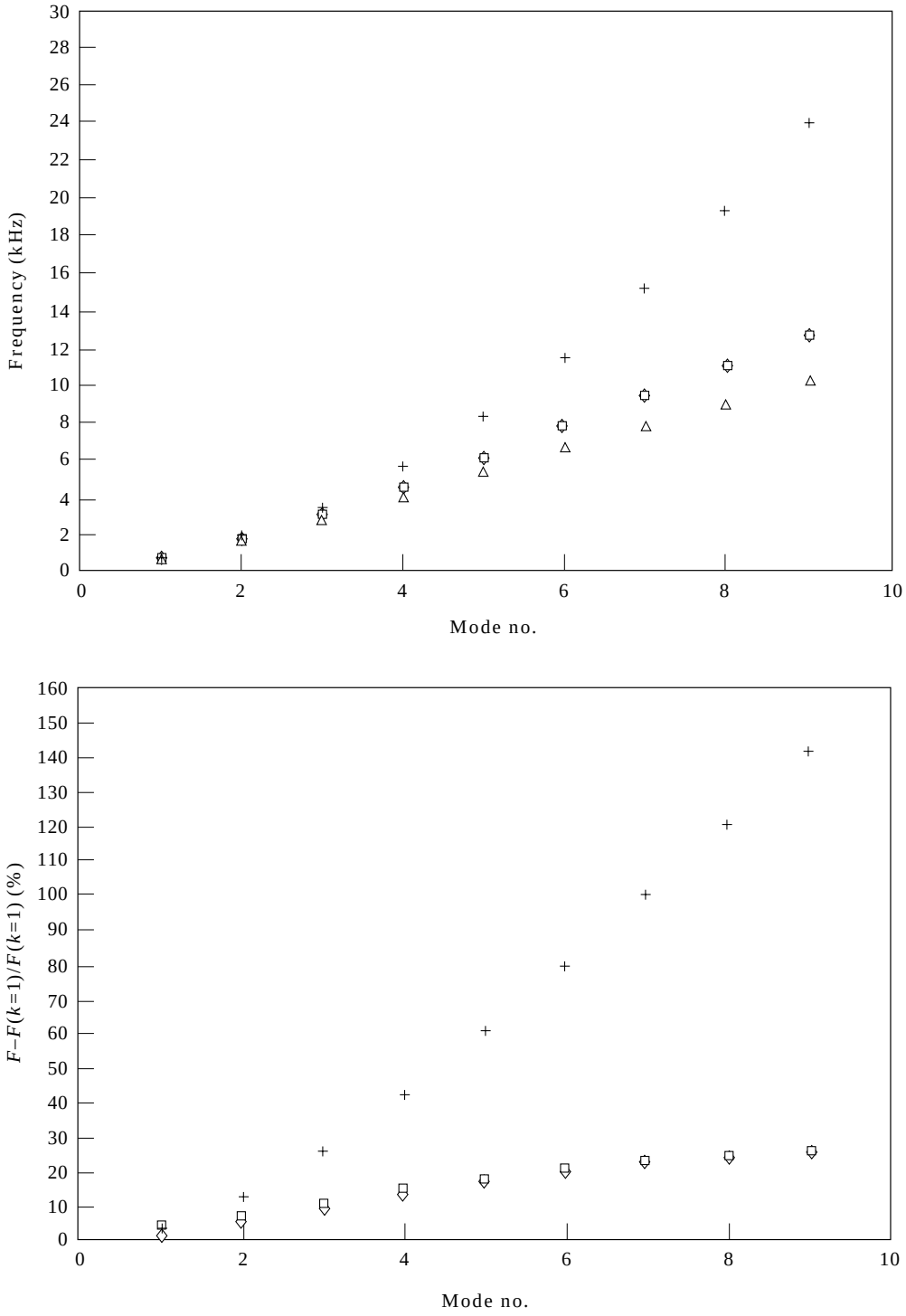

Figure 6. Frequency versus mode no. (test piece: SB1, 0·5 in. thick M-Board sandwich beam). Key as Figure 3, except ◇, Timoshenko ($k = 1{\cdot}77$).

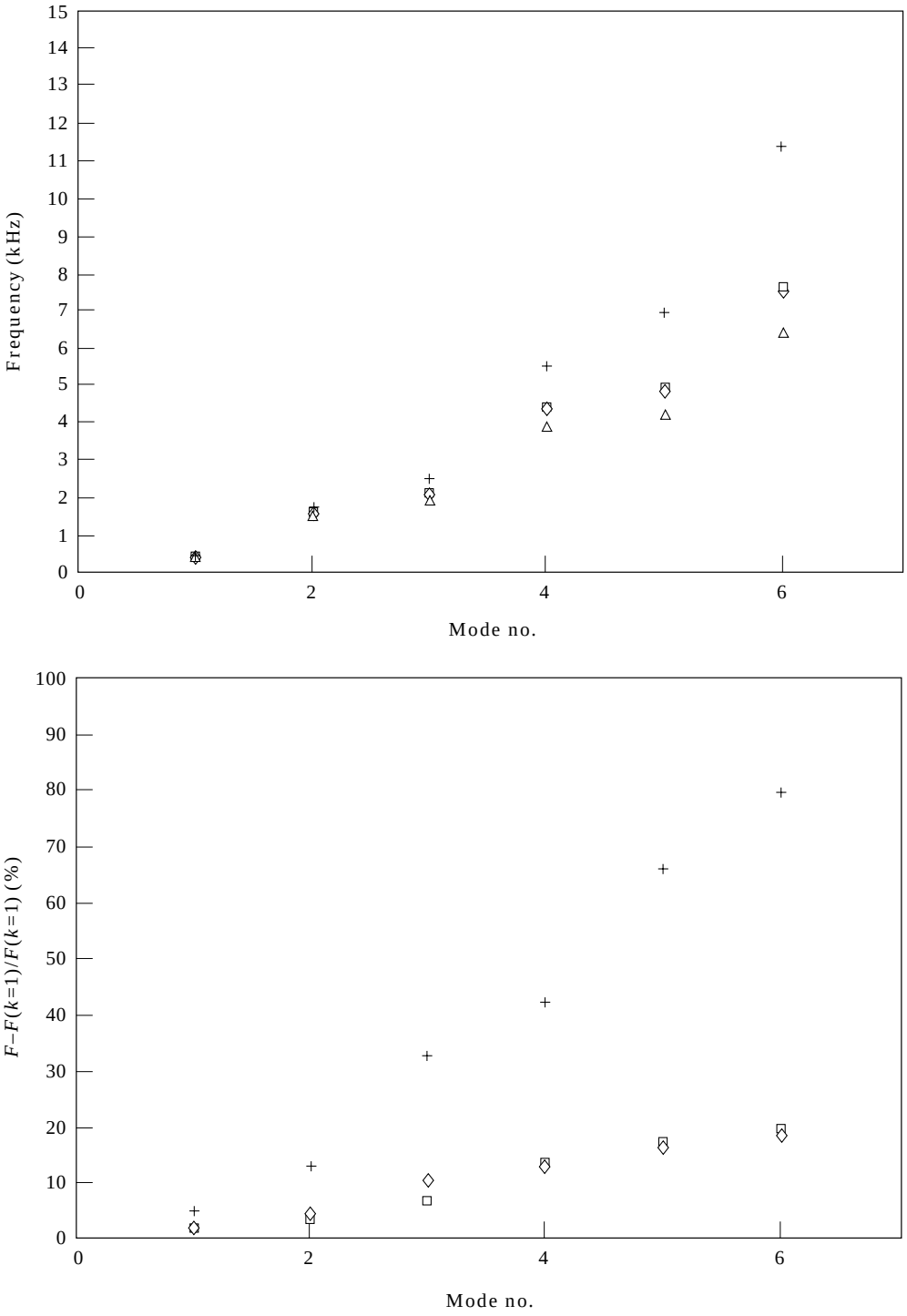

Figure 7. Frequency versus mode no. (test piece: centrally-loaded SB1, 0·5 in. thick M-Board sandwich beam.) Key as Figure 6.

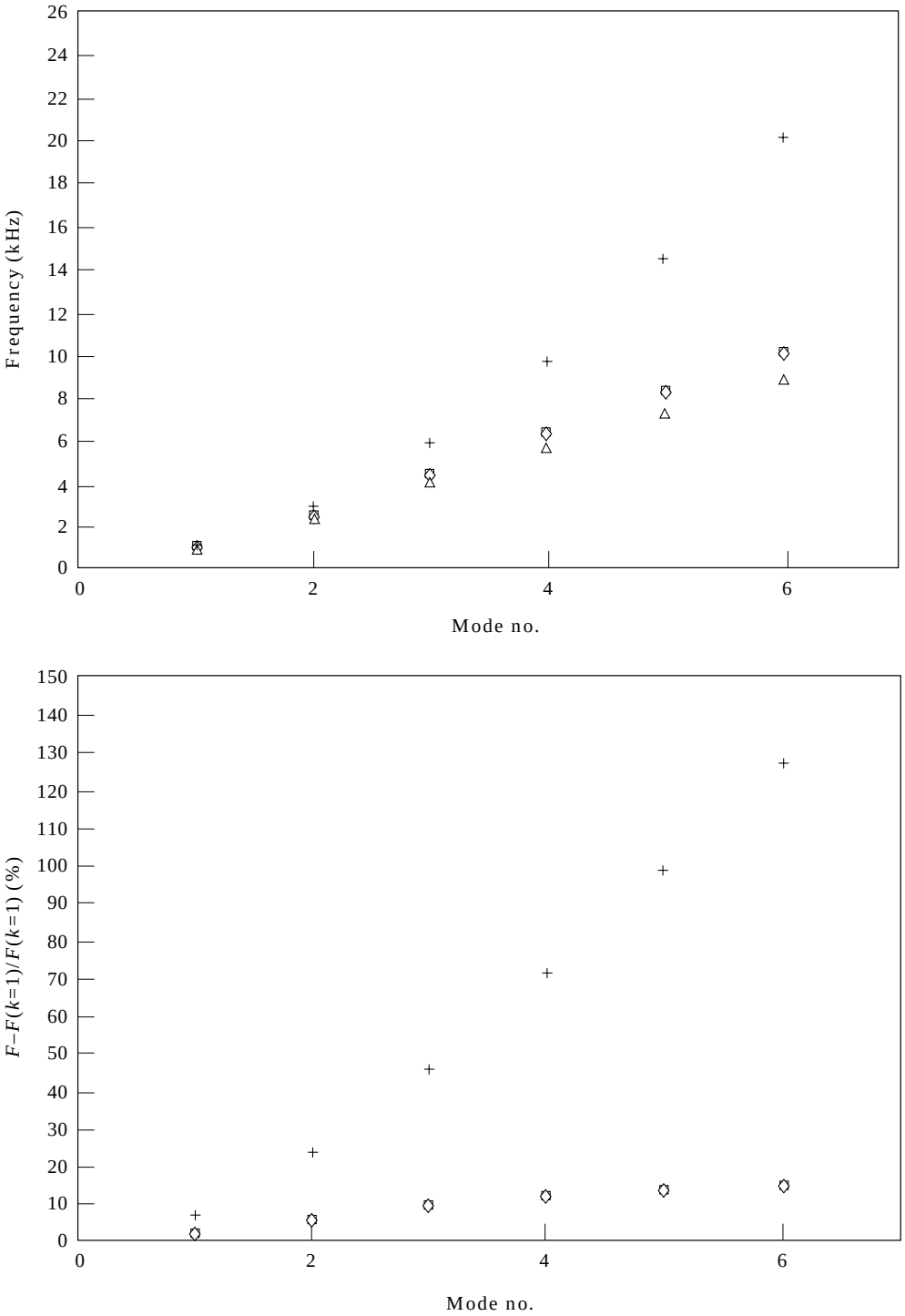

Figure 8. Frequency versus mode no. (test piece: SB2, 1 in. thick M-Board sandwich beam). Key as Figure 6, except ◇, Timoshenko ($k = 1{\cdot}42$).

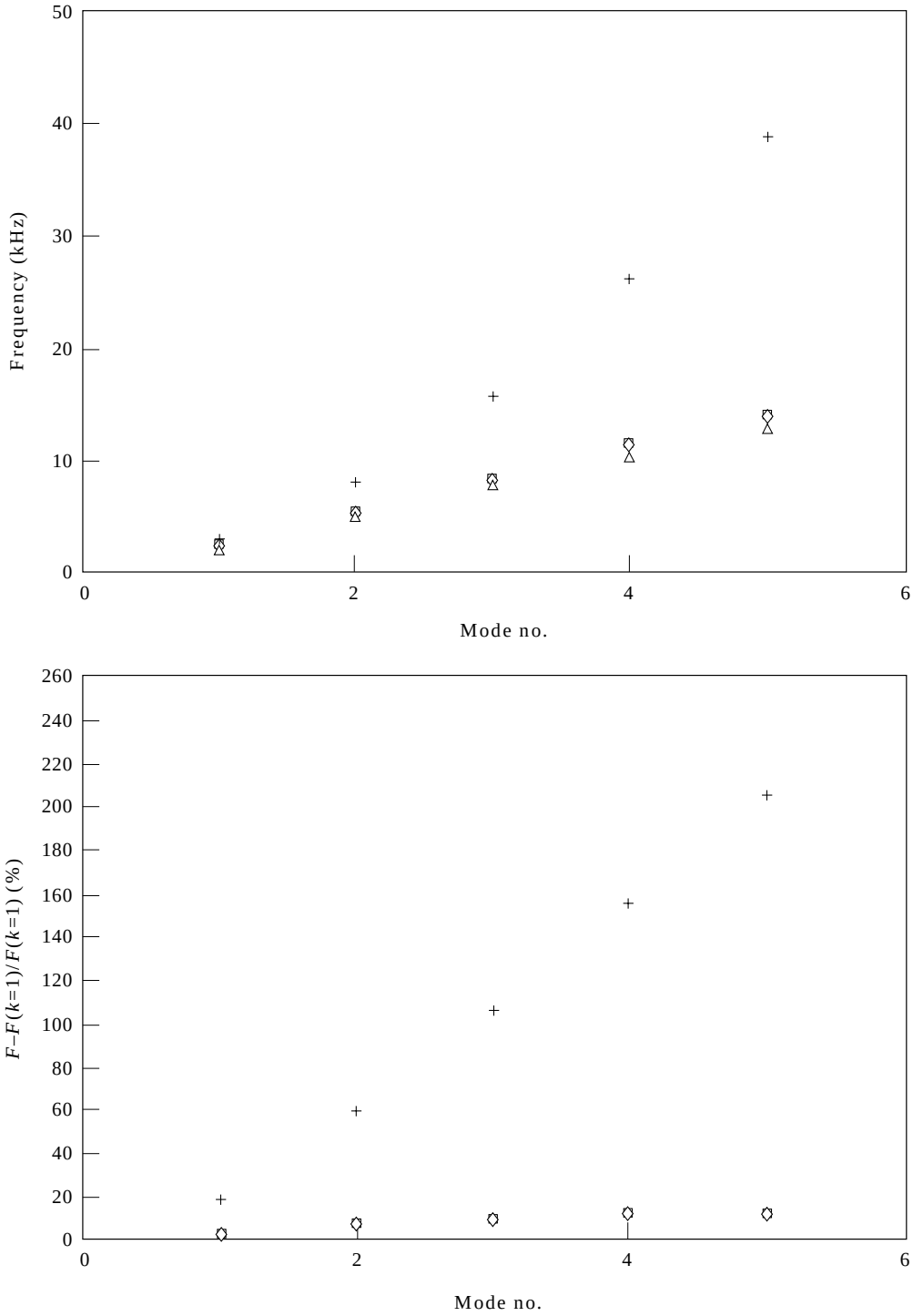

Figure 9. Frequency versus mode no. (test piece: SB3, 1·33 in. thick M-Board sandwich beam). Key as Figure 8, except ◇, Timoshenko ($k = 1{\cdot}25$).

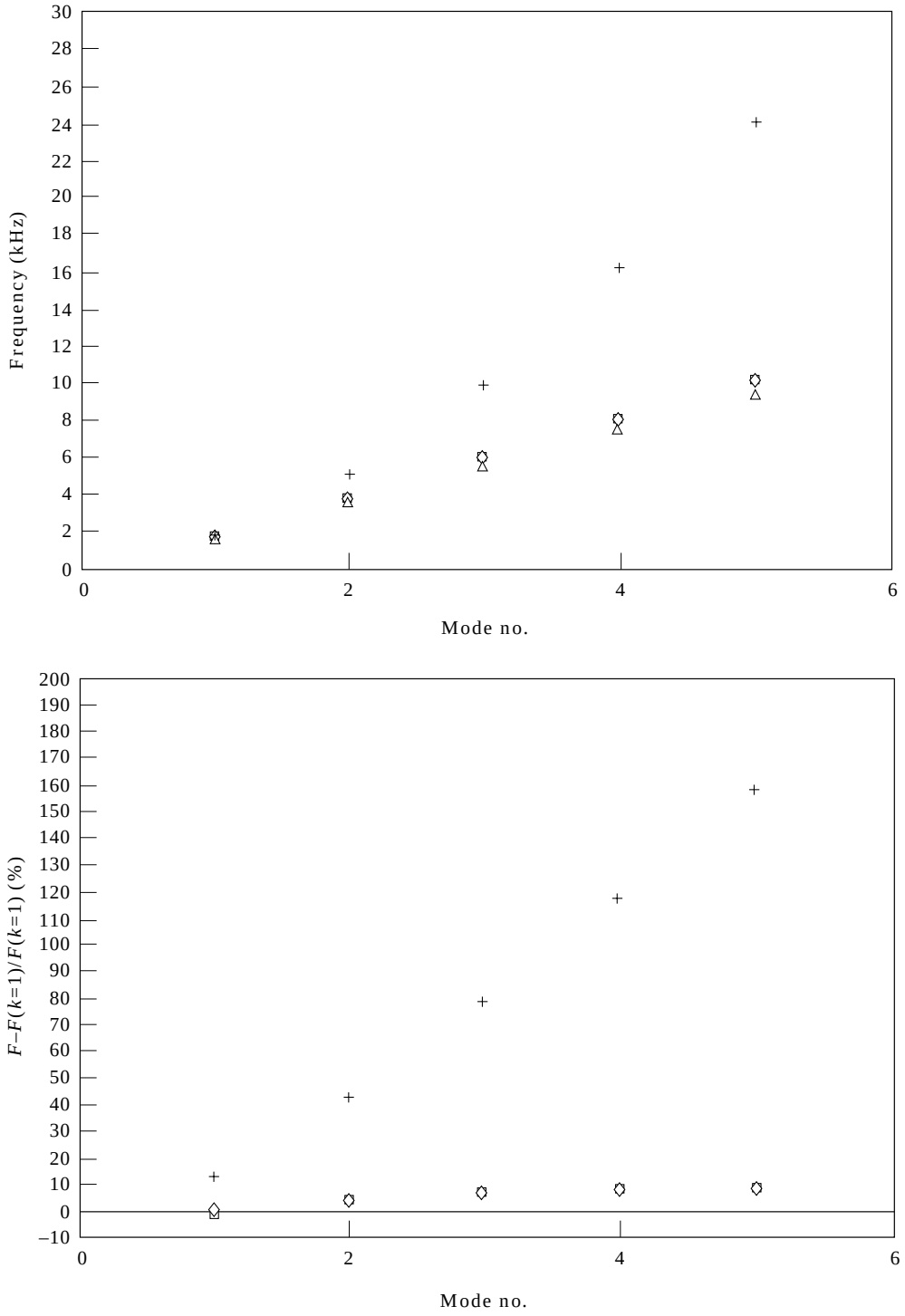

Figure 10. Frequency versus mode no. (test piece: SB4, 2 in. thick M-Board sandwich beam.) Key as Figure 9, except ◇, Timoshenko ($k = 1{\cdot}20$).

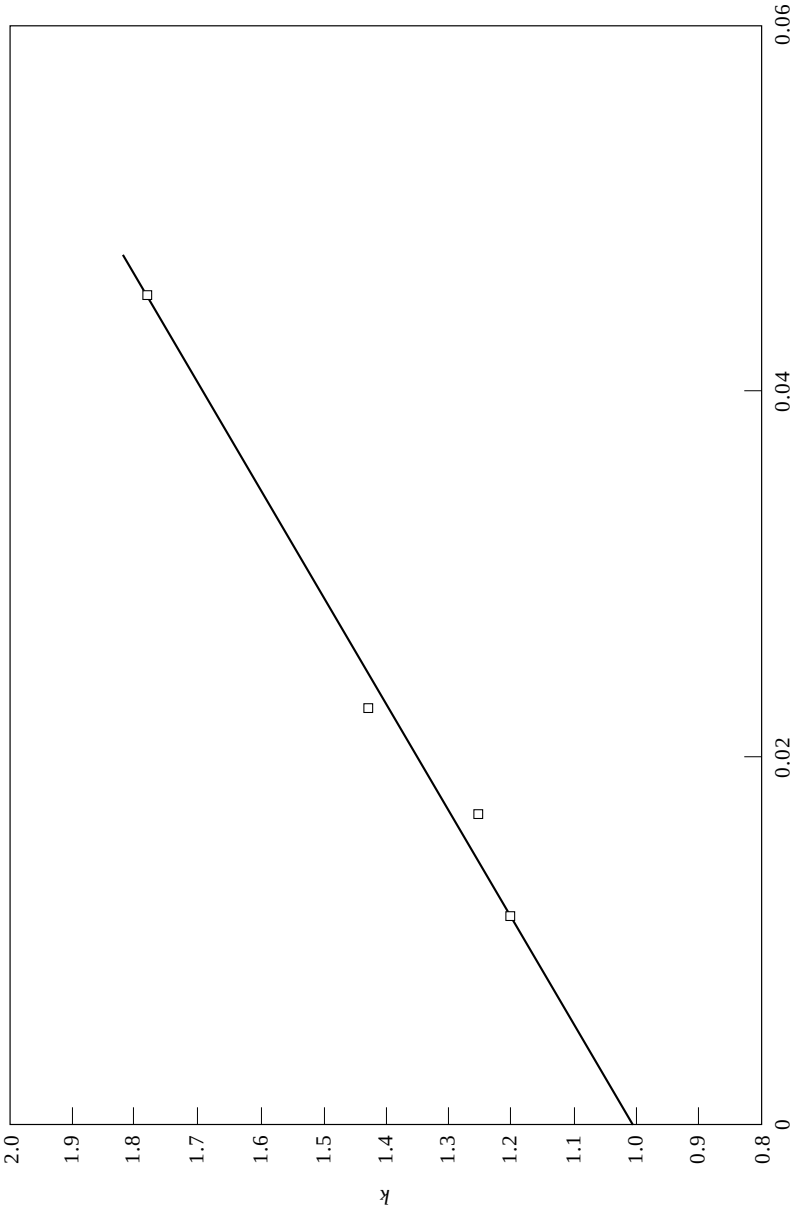

Figure 11. Optimum shear factor versus skin/core thickness.

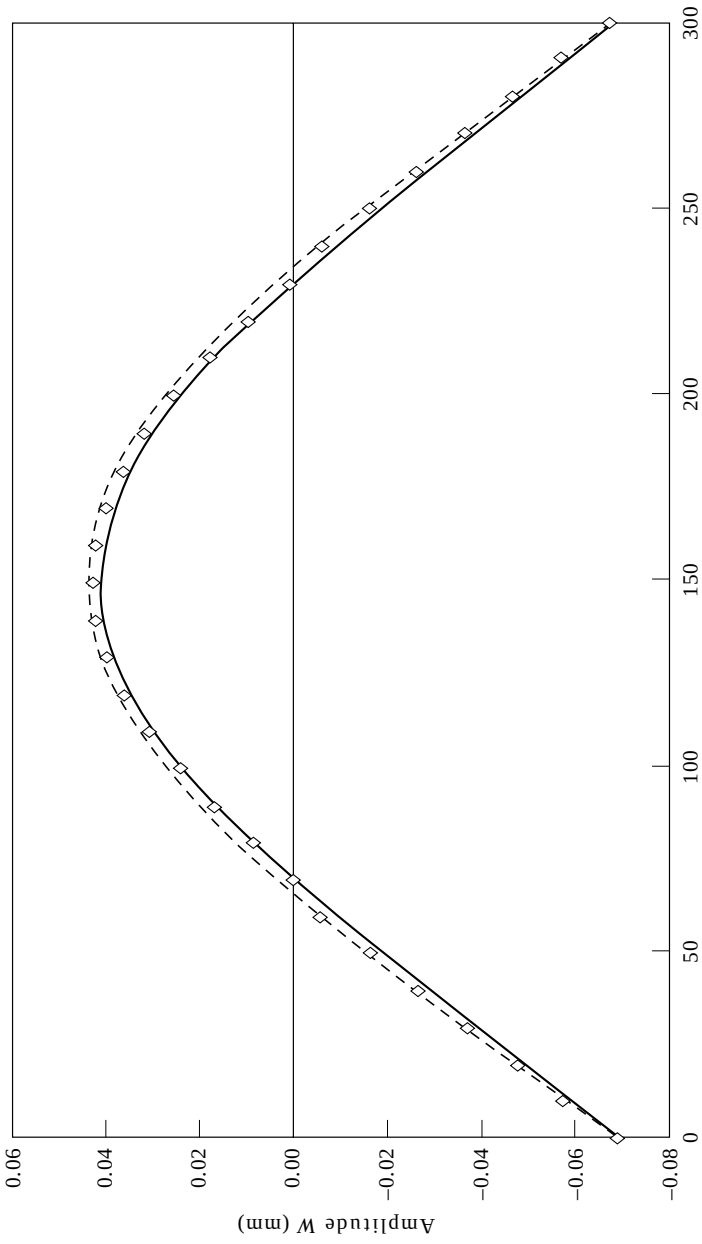

Figure 12. Mode shape of SB1 (free–free, unloaded, 300 mm). ◇, Test; ——, Timoshenko ($k = 1$); – – –, Bernouilli–Euler.

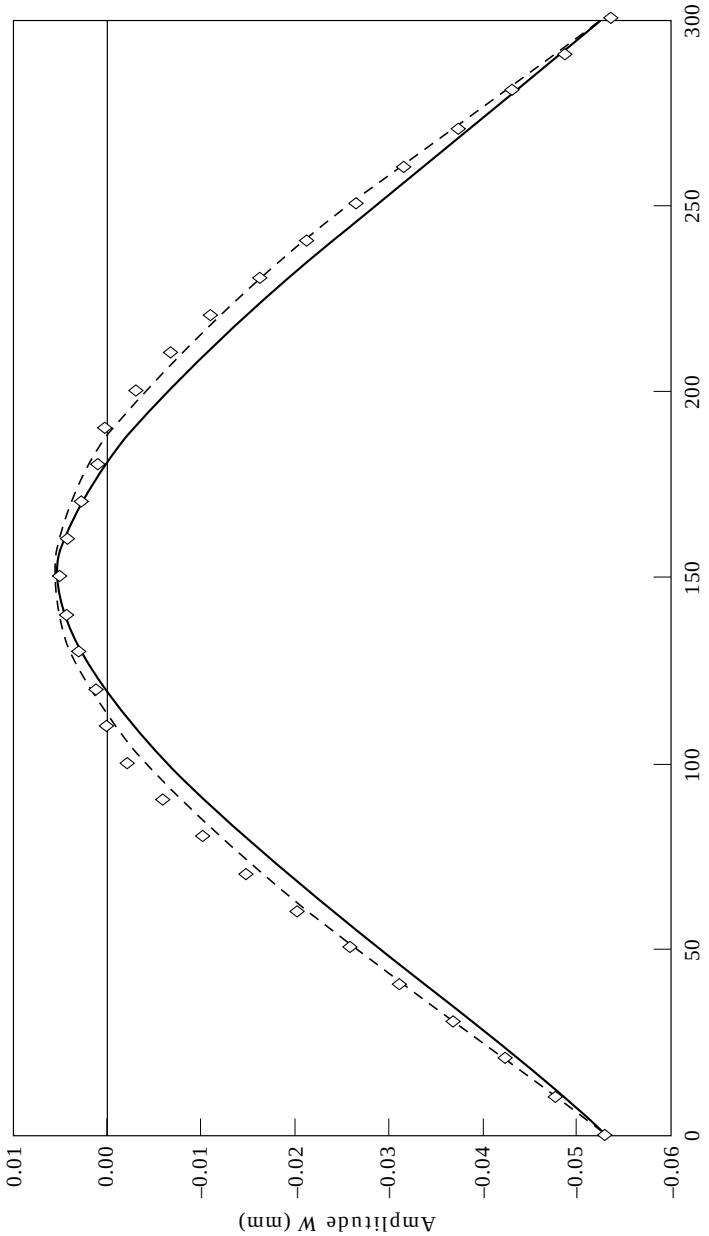

Figure 13. Mode shape of SB1 (free–free, centrally loaded, 300 mm). Key as Figure 12.

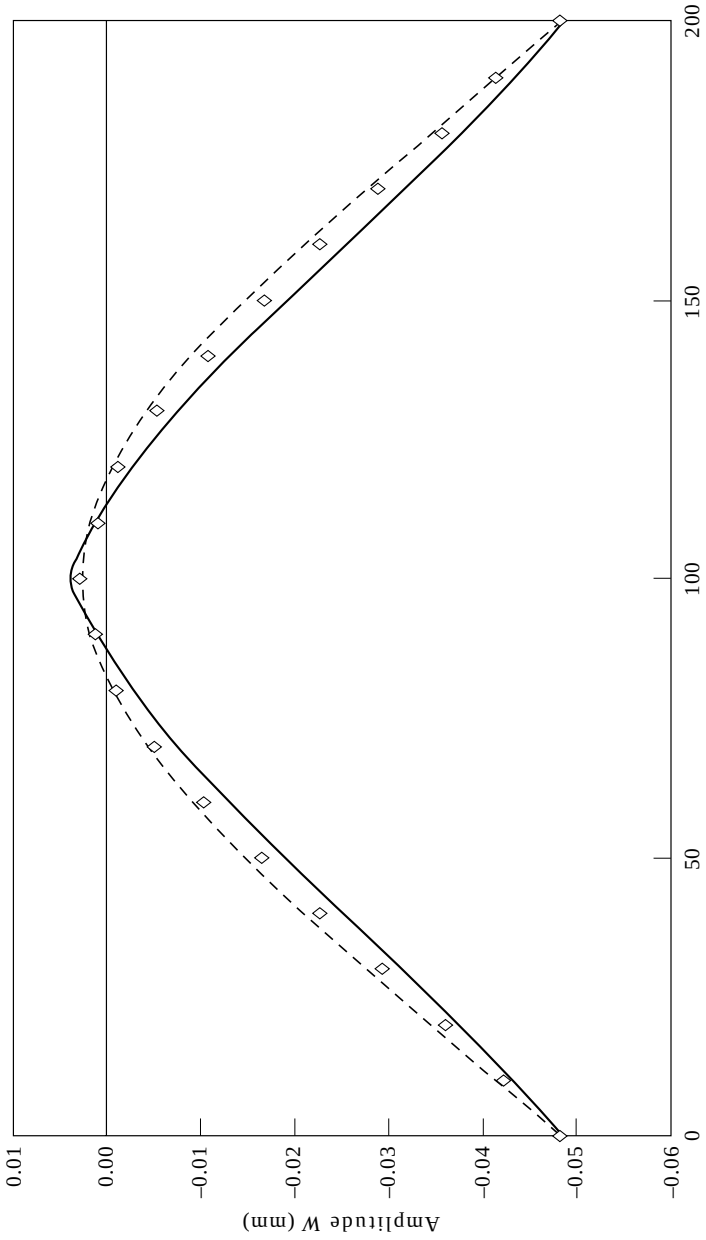

Figure 14. Mode shape of SB1 (free–free, centrally loaded, 200 mm). Key as Figure 12.

with the ratio of skin/core thickness, and that a value of 1.0 for k occurs only for an infinitely small skin/core thickness ratio.

5.2. MODE SHAPES

A series of tests was conducted on the mode shape of the SB1 sandwich beam. All the tests were carried out in the first mode, and the beam was supported on cotton threads at the two nodal lines. Both unloaded and loaded beams were tested. In the latter case, the beam was loaded at the mid-span with the drive and pick-up coil assembly (of 134 g mass). In the case of the unloaded beams, an electrodynamic shaker was used for excitation.

Originally, an image-shearing optical device was used to measure the displacement amplitude [2]. This method, however, is only of limited accuracy given the minute displacement amplitude in a sandwich. In the present work, laser interferometry was used for that purpose. For each test, the displacement amplitude was measured at equal intervals (10 mm) along the beam.

The flexural mode shape (lateral displacement amplitude) results are shown in Figures 12–14, including both theoretical as well as experimental results. The theoretical mode shapes have been normalized with respect to the end displacement amplitude.

Two general trends become apparent from examining the mode shape results. First, core compression seems to occur between the nodal lines, as is immediately apparent in the case of the loaded beams (Figures 13 and 14). Closer examination of the mode shape results of the unloaded beam (Figure 12) shows that core compression also occurs in the unloaded beam, although here it is of a much more limited scale than the loaded beams.

The second trend, which is observable particularly in Figure 14, is a change in the curvature of flexure between the mid-span and the beam's end. This change in curvature is evident in both experimental as well as the Timoshenko results, but not in the shear–rigid Bernoulli–Euler mode shape where, as expected, the curvature is that of normal bending. In a shear–soft sandwich beam, there occurs a differential shearing along the beam, being zero at the mid-span, and at a maximum at the end. This appears to be responsible for the change in the curvature of flexure along the beam. The amount of shearing in the overall deformation will depend on the thickness/length ratio, the mode number and any load carried by the beam. In general, as the results in Figures 12–14 also indicate, an increase in any of these factors will result in an increase in the contribution of shear deformation, although the influence of added mass will be less at higher modes.

6. CONCLUSIONS

On the basis of the Timoshenko beam equations, the theoretical frequencies and mode shapes of both solid as well as sandwich beams were computed, and these were shown to follow reasonably well the experimental results. In the case of solid beams, it was shown that any difference in predictions due to using different proposed values of k is marginal and well within the limitations of an experimental verification. In the case of the sandwich beams, the factor k was chosen to fit the experimental data at the high frequency end, whereupon close agreement was found between the experimental and theoretical frequencies over the entire frequency range considered. It was concluded that the factor k was a linear function of the relative thickness of the skin and of the core, and that in practical situations its value was more than unity. Core compression between the nodal

lines was evident in the sandwich beams, and this seemed to increase with increase in shear. Otherwise, the trend of the experimental mode shapes correlated reasonably well with that of a Timoshenko beam.

REFERENCES

1. R. D. Adams and D. G. C. Bacon 1973 *Journal of Physics* D: *Applied Physics* **6**, 27–41. Measurement of the flexural damping and Young's modulus of metals and reinforced plastics.
2. M. R. Maheri 1991 *PhD Thesis*, *Department of Mechanical Engineering*, *University of Bristol*. Vibration damping in composite/honeycomb sandwich beams.
3. C. W. Bert, D. J. Wilkins and W. C. Crisman 1967 *Journal of Engineering for Industry*, *Transactions of the ASME* **89B**, 662–670. Damping in sandwich beams with shear flexible cores.
4. I. G. Ritchie 1973 *Journal of Sound and Vibration* **31**, 453–468. Improved resonant bar techniques for the measurement of dynamic elastic moduli and a test of the Timoshenko beam theory.
5. S. Timoshenko 1955 *Vibration Problems in Engineering* (third edition). London: Macmillan Company, Ltd.
6. T. C. Huang 1961 *Journal of Applied Mechanics*, *Transactions of the ASME* **83**, 571–584. The effect of rotatory inertia and of shear deformation on the frequency and normal mode equations of uniform beams with simple end conditions.
7. W. L. James 1962 *Report No*. 1888, *Forest Products Laboratory*, *Madison*, *Wisconsin*. Calculation of vibration damping in sandwich construction from damping properties of the cores and the facings.
8. R. A. DiTaranto 1965 *Journal of Applied Mechanics*, *Transactions of the ASME* **87(E)**, 881–886. Theory of vibratory bending for elastic and viscoelastic layered finite-length beams.
9. D. J. Mead and S. Markus 1969 *Journal of Sound and Vibration* **10**, 163–175. The forced vibration of a three-layered, damped sandwich beam with arbitrary boundary conditions.
10. L. H. Donnell 1976 *Beams*, *Plates*, *and Shells*. London: McGraw-Hill Book Company.
11. T. S. Chow 1971 *Journal of Composite Materials* **5**, 306–319. On the propagation of flexural waves in an orthotropic laminated plate and its response to an impulsive load.
12. D. J. Mead 1982 *Journal of Sound and Vibration* **83**, 363–377. A comparison of some equations for the flexural vibration of damped sandwich beams.
13. S. Timoshenko and J. N. Goodier 1951 *Theory of elasticity* (second edition). London: McGraw-Hill Book Company.
14. L. E. Goodman 1954 *Journal of Applied Mechanics*, *Transactions of the ASME* **76**, 202–204. Discussion of paper (R. A. Anderson, 1953).
15. R. D. Mindlin and H. Deresiewicz 1955 *Proceedings of the 2nd U.S. National Congress on Applied Mechanics*, 171–178. Timoshenko's shear coefficient for flexural vibrations of beams.
16. Y.-Y. Yu 1959 *Journal of Applied Mechanics*, *Transactions of the ASME* **26**, 679–681. Simple thickness-shear modes of vibration of infinite sandwich plates.
17. R. D. Adams and M. R. Maheri 1993 *Composites Science and Technology* **47**, 15–23. The dynamic shear properties of structural honeycomb materials.
18. R. D. Mindlin 1951 *Journal of Applied Mechanics* **8**, 31–38. Influence of rotatory inertia and shear on flexural motions of isotropic, elastic plates.

APPENDIX: NOMENCLATURE

A cross-sectional area of solid beam
cross-sectional area of sandwich core
b frequency number
c thickness of sandwich core
E Young's modulus
E_s Young's modulus of sandwich skin
F natural frequency
G shear modulus
G_c shear modulus of sandwich core
h depth of solid beam
I area moment of inertia

J polar mass moment of inertia
k shear shape correction factor
L length of beam
M_c central mass attached to the beam
m mass of beam
r rotary inertia parameter
s shear flexibility parameter
t thickness of sandwich skin; time
W total lateral deflection
w time dependent total lateral deflection; width of beam
x distance along the beam
γ shear rotation
Φ bending slope
ϕ time dependent bending slope
ρ mass density
ν Poisson's ratio
ω natural angular frequency